GODDARD SPACE FLIGHT CENTER

Evaluation Report

Microcircuit (10)
Mfr.: MICREL
P/N: SY89424VZC
D/C: 9910

Project
VCL
System
Parts testing
Requester
K.Sahu (562)

Malfunction Report

Incoming Inspected

Initiated Date
10/01/00

Purchase Specifications
commercial

Screening Specifications
commercial

Investigator
A.Teverovsky (562)

Approval for Distribution/Date

_____

Background

Ten MICREL SY89424VZC commercial microcircuits proposed for the VCL project were submitted to the GSFC Parts Analysis Laboratory for evaluation of their design, materials and potential risk for long term reliability.

Part Description

The SY89424VZC is a low power PLL based frequency synthesizer which is capable of generating up to 1GHz clock frequencies. The part is encapsulated in a standard surface mount 16-lead plastic package (SOIC, type Z16-1). An operating temperature range for the part is 0 °C to +75 °C and a storage temperature range is –65 °C to +150 °C.

Analysis.

1. External and Radiographic Examinations.

External examination showed that the part had no package warping, cracks, voids, or foreign inclusions in the plastic encapsulant. One sample had a minor chip-out at the package edge, however, this defect can be considered as minor. No gaps were observed between the entry of the leads and the molding compound (MC). Figure 1 gives external views of the part.

Radiographic examination showed adequate wire bond dressing. Typical top and side X-ray views of the part are displayed in Figure 2.

2. Scanning Acoustic Microscopy.

2.1. Reflow simulation.

Top and bottom sides of the die/lead frame assembly in five parts were examined using an acoustic microscope (C-SAM mode with a 15 MHz transducer) before and after solder heat resistance simulation. This simulation was performed by immersing the parts in a solder pot at 245 ± 5 °C for 5 seconds and then spray cleaned with isopropanol. This procedure was repeated three times.

Initial C-SAM examination showed (see Figures 3 and 4) that three out of five parts had partial delamination at the paddle-molding compound interface. External visual examination after solder pot simulation did not reveal any defects. However, acoustic microscopy showed that after the test all parts had entire paddle area delaminated and, what is more important, in one part, SN 2, an interfacial gap had been formed on the die surface. Also, three parts (SNs 1, 2, 3) had delaminations at the lead tips, where the wires are crescent bonded to the lead frame.

Acoustic inspection of the bottom side also revealed an increase of delaminated area at the paddle back side-molding compound interface (see Figure 4).

2.2. Temperature cycling of DPA parts.

Two parts after solder heat resistance simulation and three new parts were subjected to 100 temperature cycles between –65 °C and +150 °C with 15-minute dwell time. Acoustic images of the parts before and after temperature cycling are shown in Figures 5 and 6.

In the new parts delamination at the top-side paddle-MC interface was increased to 100% of the available area. However, no defects were observed on the die surface and on the lead tips. Two previously stressed parts (SN 4 and 5) had an increased area of delamination at the lead tips.

Temperature cycling resulted in an increase of delaminated area at the paddle back side in only one part, SN 10.

Electrical testing of samples SN 6, 7, and 10, at room temperature did not reveal any anomaly.

2.3. Temperature cycling of flight parts.

The above results suggest that the part might have problems when subjected to severe thermo-mechanical stresses. To pick up the best candidates for future space applications, C-SAM examinations were performed on ten microcircuits before and after 20 temperature cycles performed at a typical for commercial microcircuits range of temperatures of –20 °C to +85 °C. The results of the test (see Figure 7) showed the following:

1. All parts except SN 53 exhibited delamination of different degree at the top-side of the paddle-molding compound interface.
2. None of the parts had delamination at the critical locations (die surface and lead frame tips) neither before nor after temperature cycling.
3. Anomalies observed on most of the parts at pins 6 and 9 were caused by triple wire bonding at these pins and were not most likely due to voiding.
4. Temperature cycling resulted in some increase in delaminated area in all parts (except SN 53 where no delamination was observed). In all cases except for SN 52 these changes can be considered as minor.
5. The best part for future applications is SN 53. All other parts, except for SN 52, were similar and demonstrated adequate stability at normal temperature cycling conditions.

3. Internal Examinations.

Two samples were decapsulated in red fuming nitric acid and examined under lower and high power optical microscope. Figure 8 shows overall view of the part after decapsulation and Figure 9 shows marking on the die. One of the dice had a mechanical damage on the surface (see Figure 10) which is rejectable per MIL-STD-883, TM2010.

4. Bond Pull Test.

All 22 wires in one sample and 16 wires in another were subjected to wire pull testing. Both parts passed the test according to MIL-STD-883, TM 2011 (2.5 g-f for 1.2 mil gold wires). The average bond pull force was 12.2 g-f with a standard deviation of 1.44 g-f in one part and 12.6 g-f and 1.98 g-f respectively for another part.

5. Glassivation integrity.

This examination was performed on one sample per MIL-STD-883D, Method 2021, "Glassivation layer integrity". The test involved a high-power optical examination after the die was subjected to aluminum etch. Aluminum etching revealed one crack in the glassivation (see Figure 11). However, detailed SEM examination of the glassivation in another part did not reveal any defects. Figure 12 shows typical SEM view of the glassivation.

6. SEM inspection of metallization.

The quality of metallization was inspected in one sample per MIL-STD-883D, Method 2018 (see Figures 13 and 14). The part has two metallization levels. No patterning or step coverage problems were found in either the top or the bottom metallization layers.

7. Package-level Cross Sectional Examinations.

One sample was cross-sectioned at several planes to examine interfaces between the molding compound and the die assembly. Figure 15 shows an overall view of the package cross section and Figures 16 and 17 show close-up views of different interfaces in the part.

The molding compound had no internal cracks or voids and formed intimate contacts to all internal surfaces (die, wires, and lead frame). No delaminations between the glassivation and the molding compound were observed.

The die was mounted to the lead frame base with a thin layer of silver epoxy. The adhesive and silver filler were uniformly distributed along the die-paddle interface. Ball bond cross sectioning showed the formation of an adequate Au/Al intermetallic layer of 2 - 3 μm in thickness (see Figure 18).

Conclusion.

Evaluation of the MICREL SY89424VZC commercial microcircuit showed that the parts had adequate wire bonding, die mounting and quality of metallization. The wire bonding exhibited normal alignment, dressing, mechanical strength and the formation of adequate Au/Al intermetallic alloys at the die contact pads. Cross sectioning indicated that the molding compound formed intimate contact to the leads and wires.
However several defects, which might be a reliability concern, has been revealed:

1. Internal examination of two parts showed mechanical damage to glassivation in one die and a crack in the glassivation in another die.

2. Acoustic microscopy showed partial delaminations at the top-side paddle - molding compound interface in most of the parts. SMT simulation (solder pot resistance) and temperature cycling (in the range –65 °C to +150 °C) showed an increase of delamination and its expansion to the die surface and lead tip areas which are critical to the device integrity. However, at common for the plastic parts temperature cycling range of –20 °C to +85 °C an increase in the delaminated area was observed only in one out of ten parts (at the paddle-MC interface which is not a critical area). No changes in the delaminated areas was observed in other nine parts, thus demonstrating that these parts most likely will not have mechanical integrity problems operating under normal conditions.

To ensure adequate quality of the parts for space applications, electrical testing of the lot at temperature extremes is recommended.

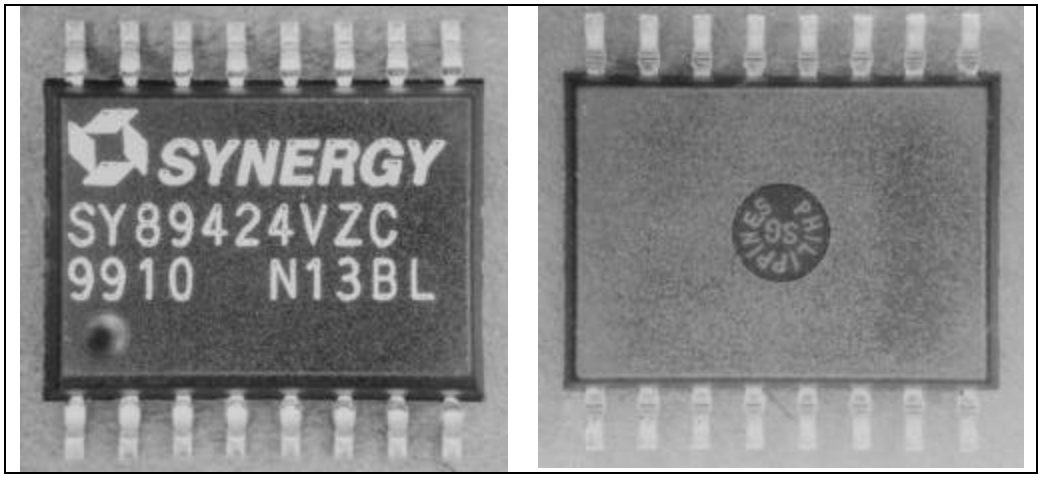

Figure 1. Top and bottom views of the part.

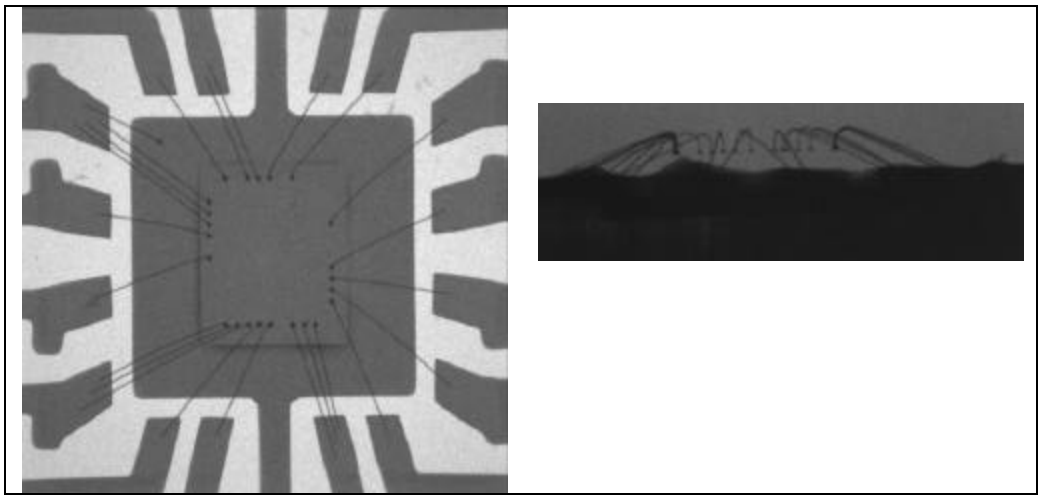

Figure 2. Typical top and side radiographic views of the part showing adequate lead frame design, wire dressing and layout.

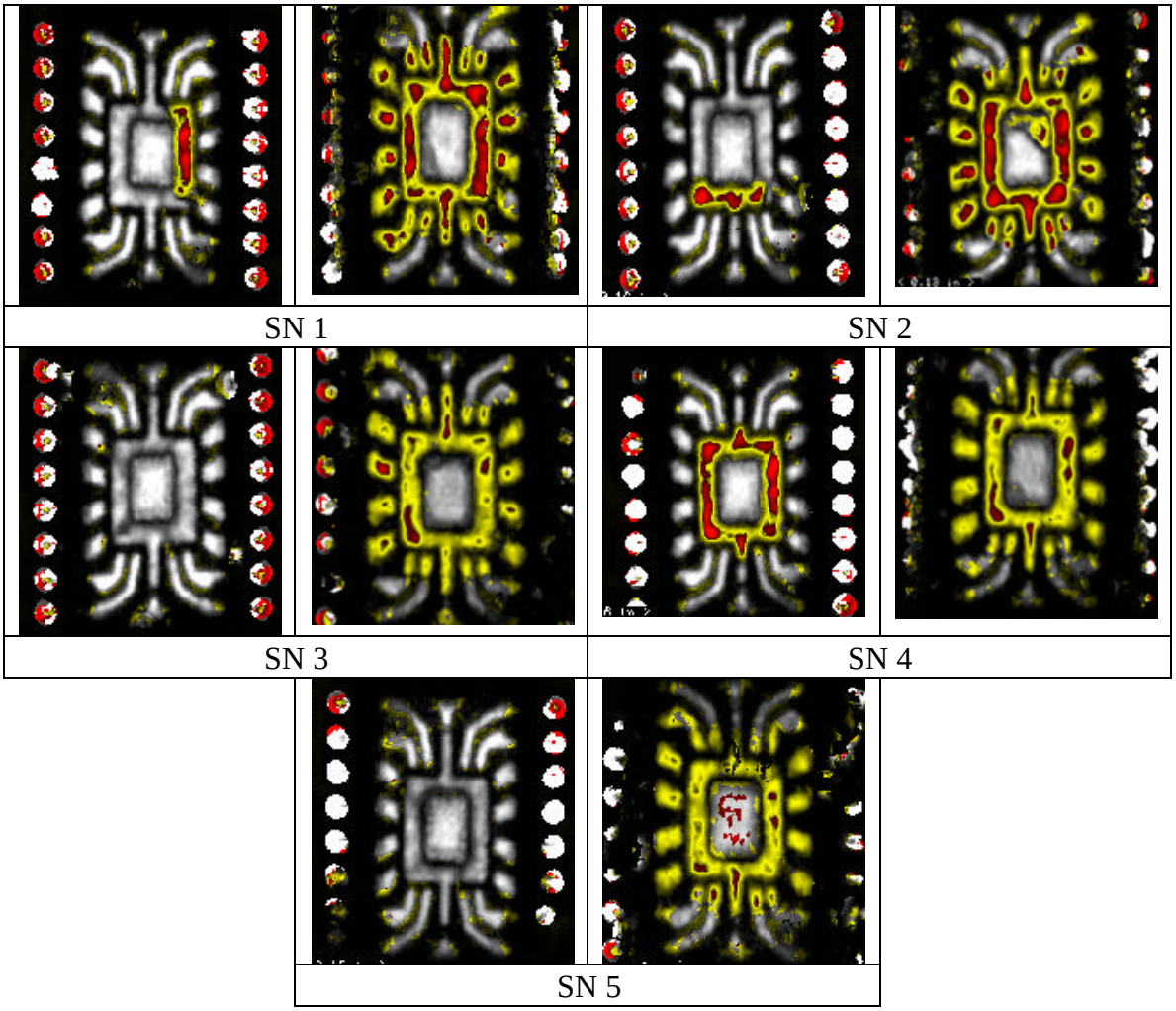

Figure 3. MICREL SY89424VZC acoustic images before (left) and after (right) solder pot test. Top side. (f = 15 MHz, Z = 21.5 us, pos. 0.489, wind. 0.4)

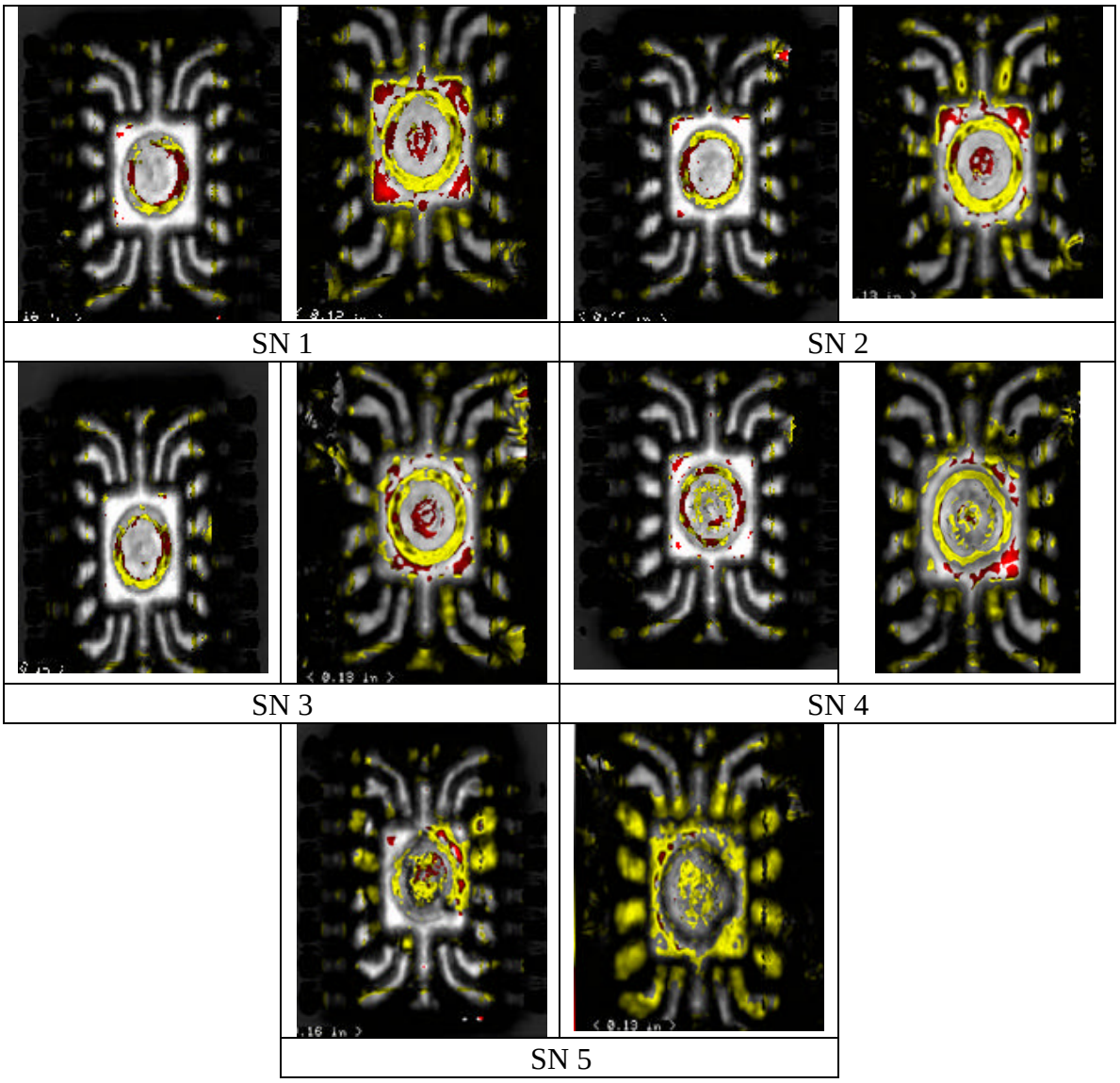

Figure 4. MICREL SY89424V acoustic images before (left) and after (right) solder pot test. Bottom side. (f = 15 MHz, Z = 21.1 us, pos. 0.431, wind. 0.3)

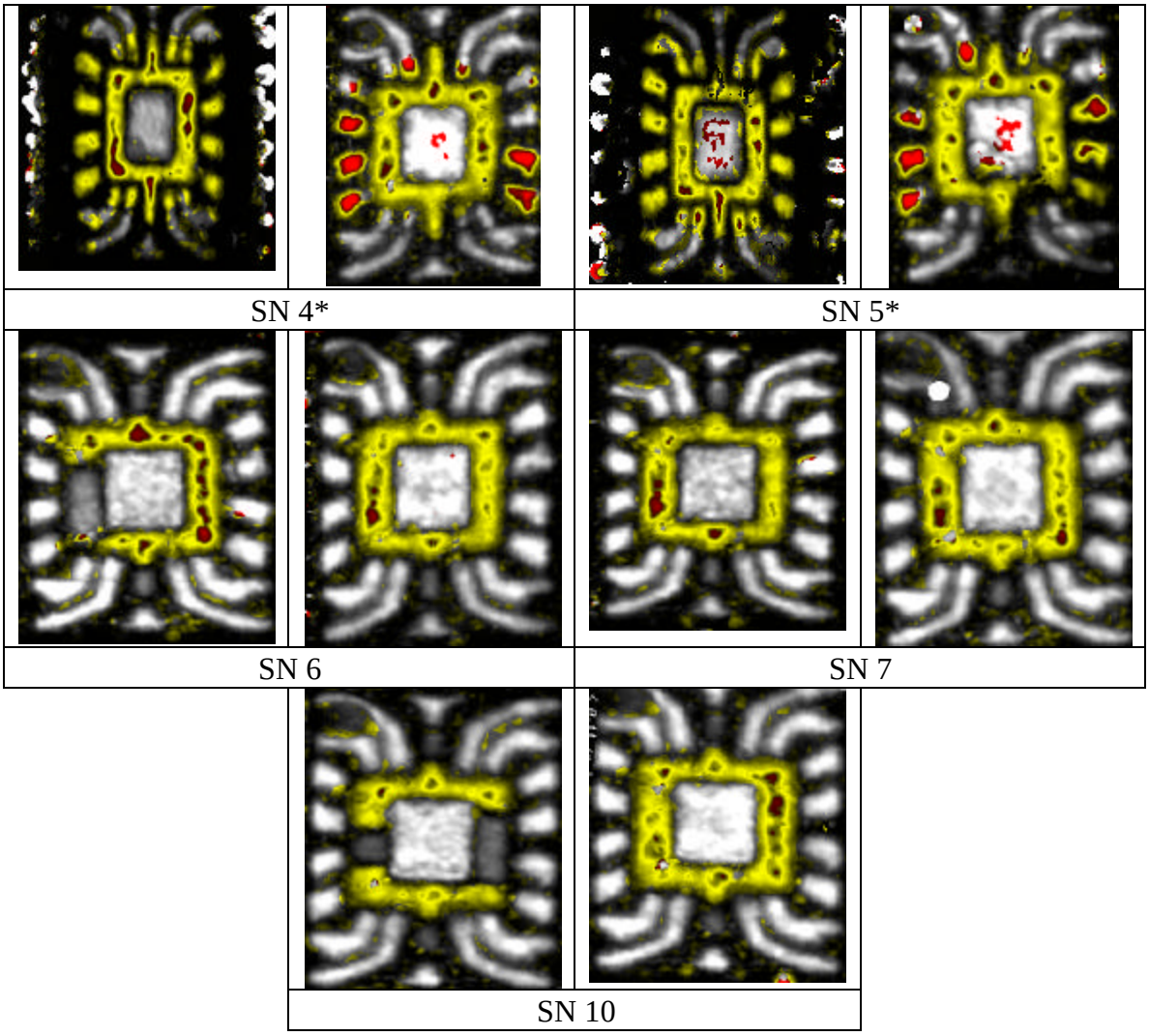

Figure 5. Acoustic images before (left) and after (right) 100 temperature cycles between –65 °C and +150 °C. Top side. Samples 4 and 5 were subjected to the solder pot test before temperature cycling.

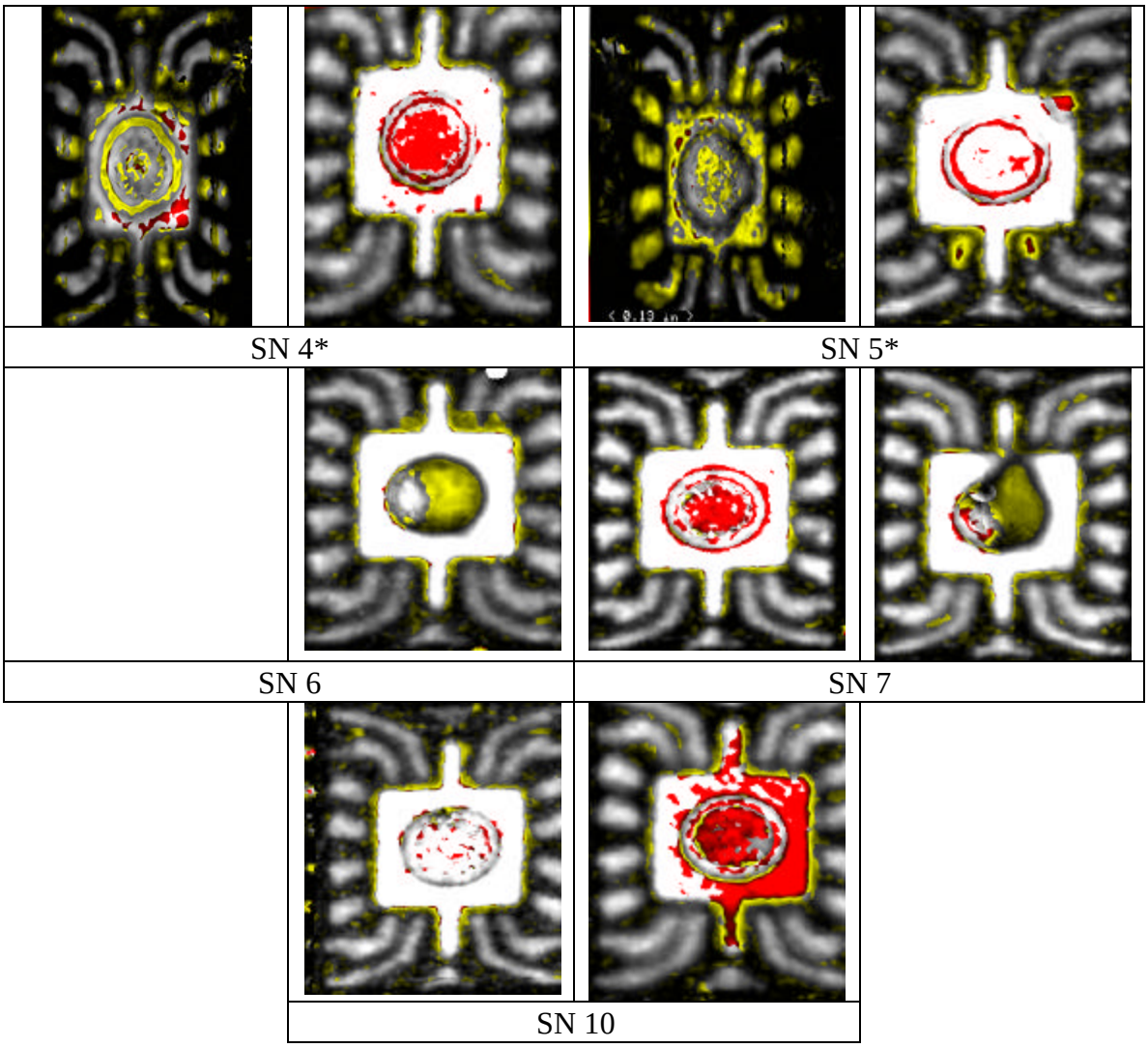

Figure 6. Acoustic images before (left) and after (right) 100 temperature cycles between –65 °C and +150 °C. Bottom side. Samples 4 and 5 were subjected to the solder pot test before temperature cycling.

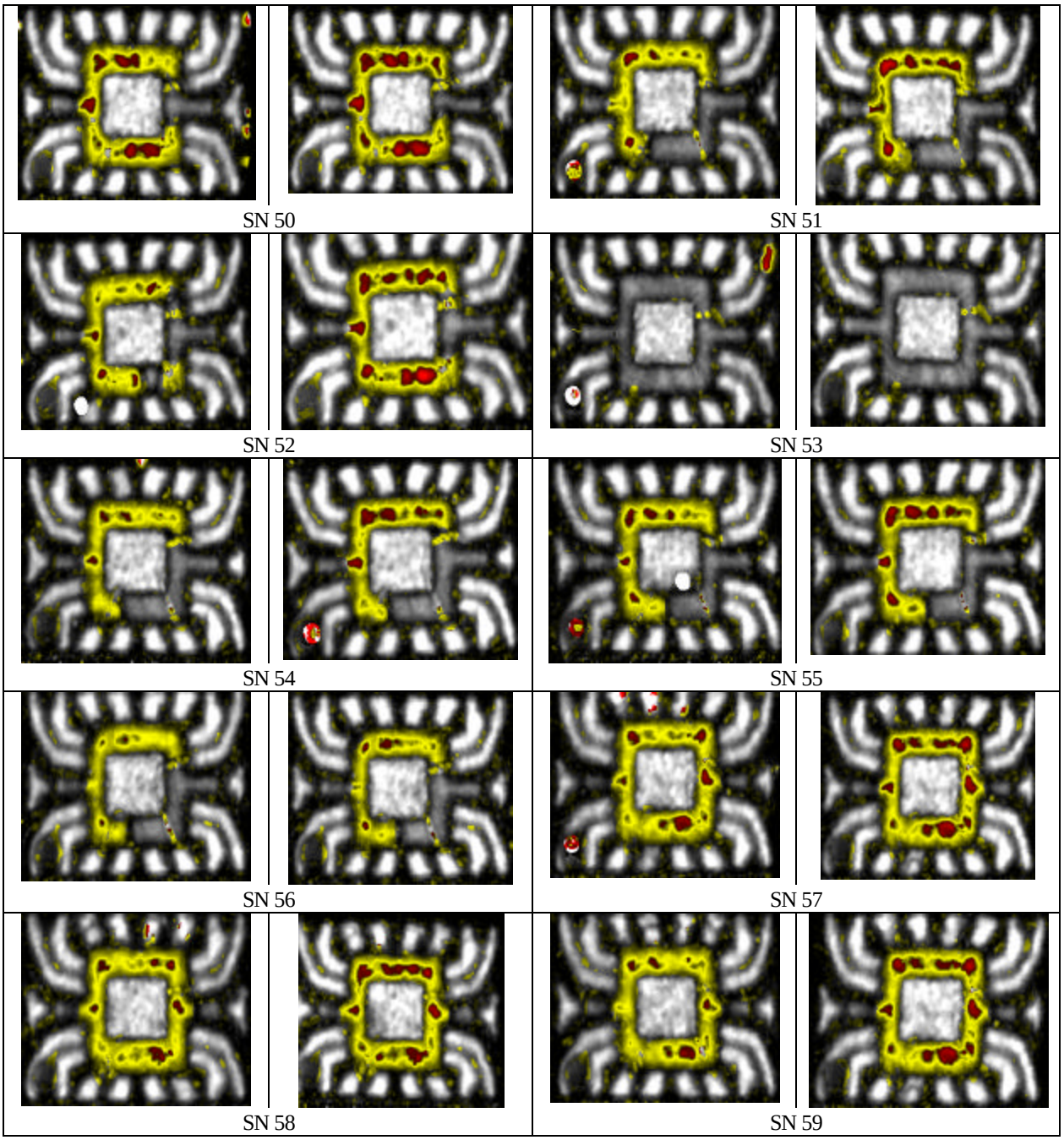

Figure 7. Acoustic images before (left) and after (right) 20 TC –20 °C to +85 °C. Top views. Pin 1 is at the left bottom corner.

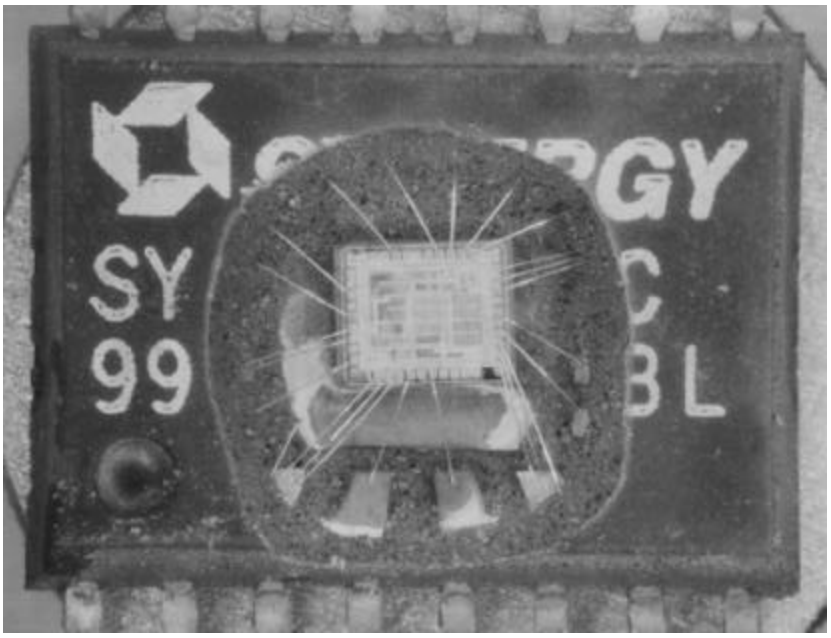

Figure 8. Overall view of the part after decapsulation.

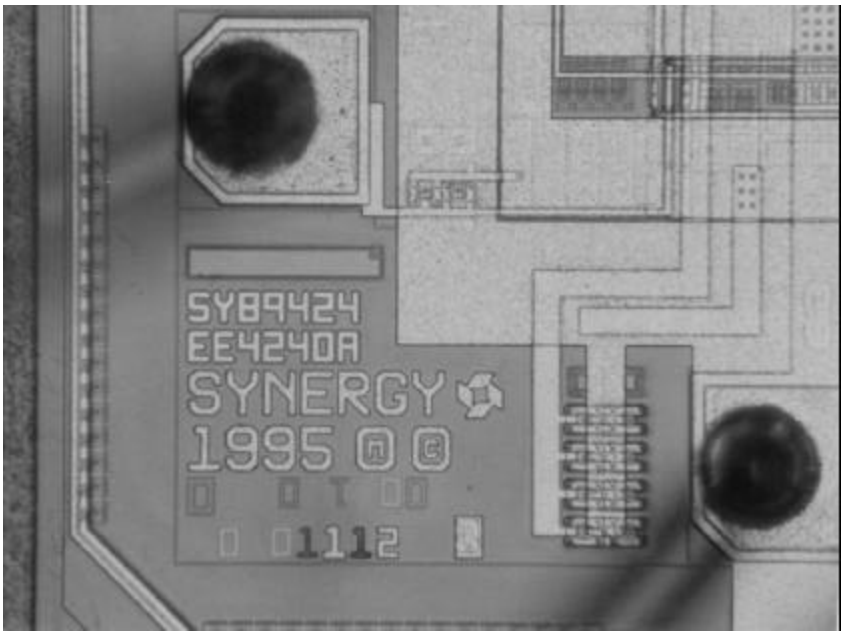

Figure 9. Marking on the die and bonds alignment. (200X)

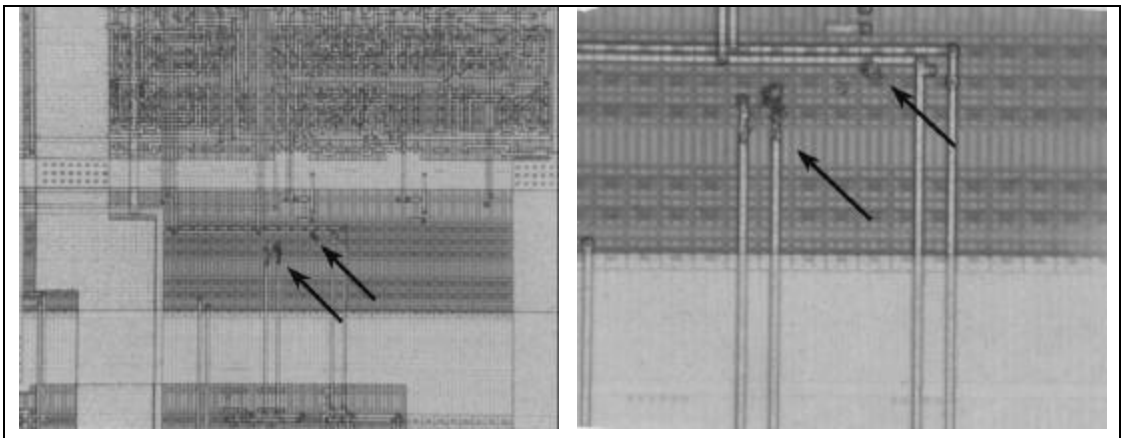

Figure 10. Mechanical damage on the die surface which prohibit inspection of the underlying metallization and thus is rejectable per MIL-STD-883, TM 2010.

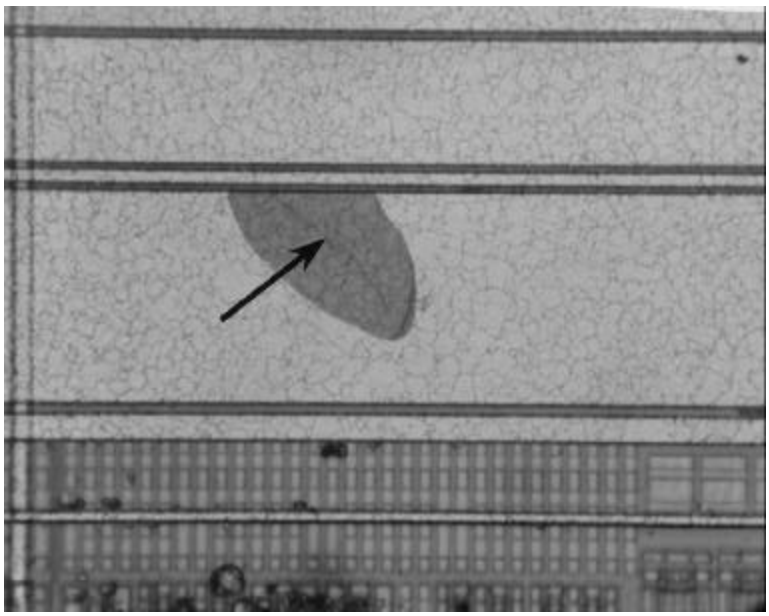

Figure 11. A crack in the glassivation revealed during the glassivation integrity test. (500X)

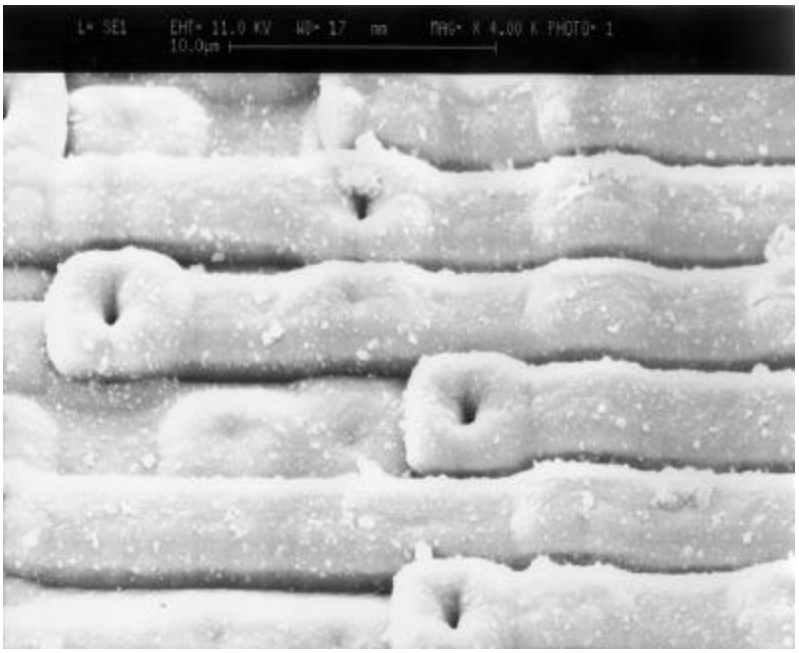

Figure 12. Typical SEM view of the glassivation (4000X)

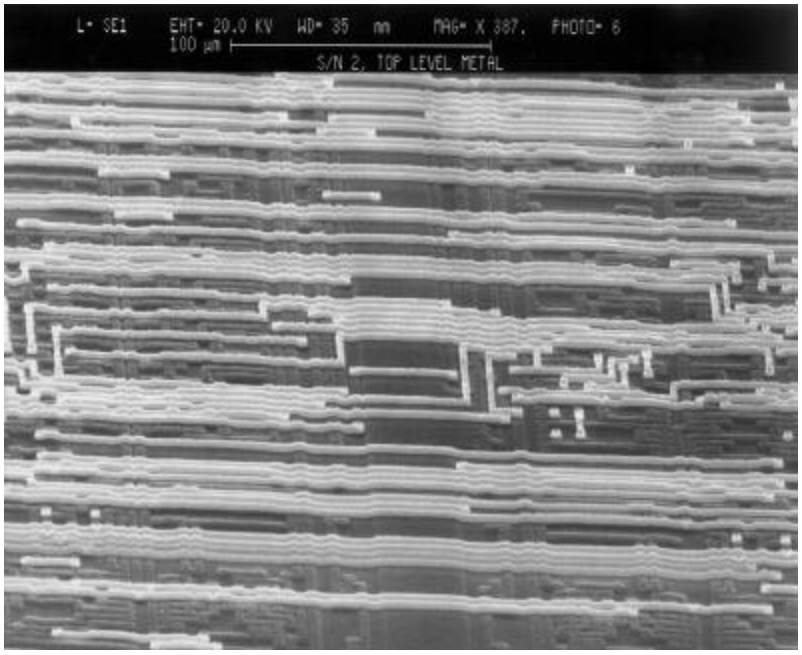

Figure 13. Overall SEM view of the die metallization. (400X)

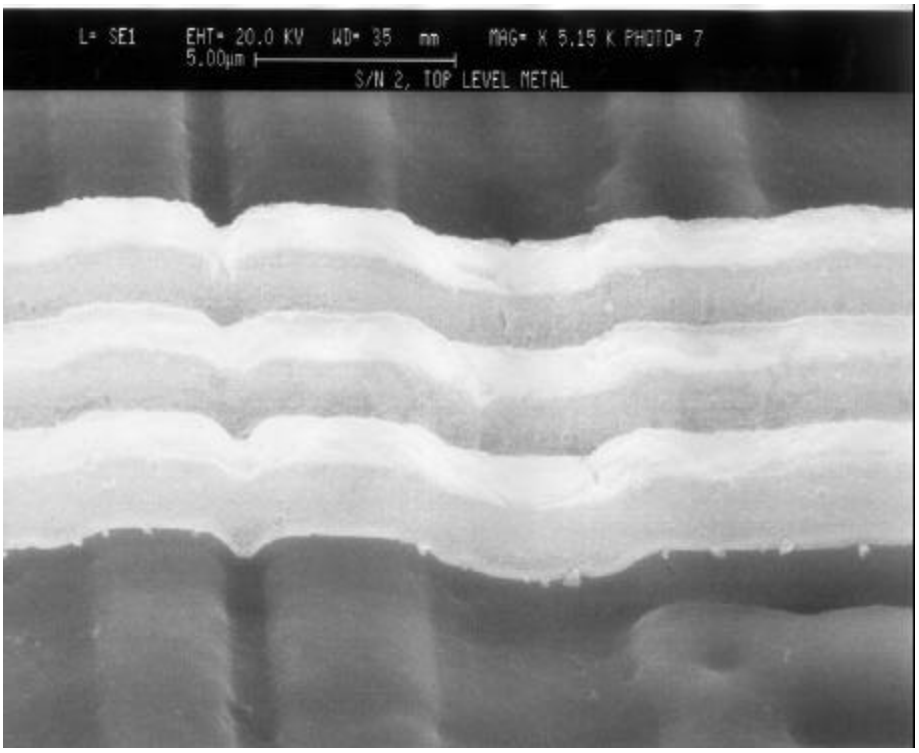

Figure 14. Close-up SEM view of the metallization. (5100X)

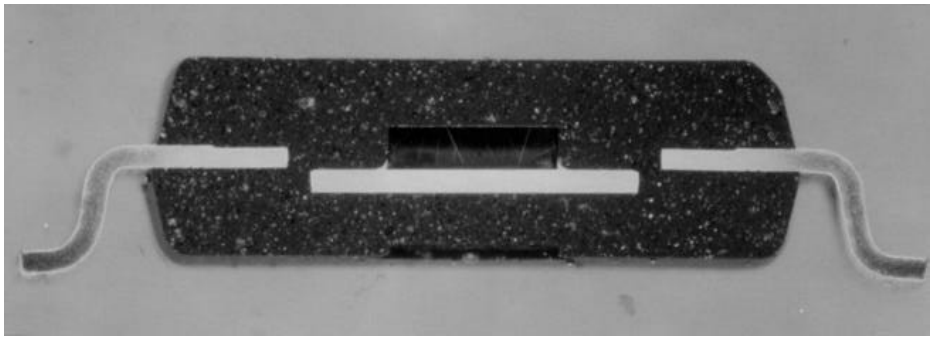

Figure 15. An overall view of the package cross section.

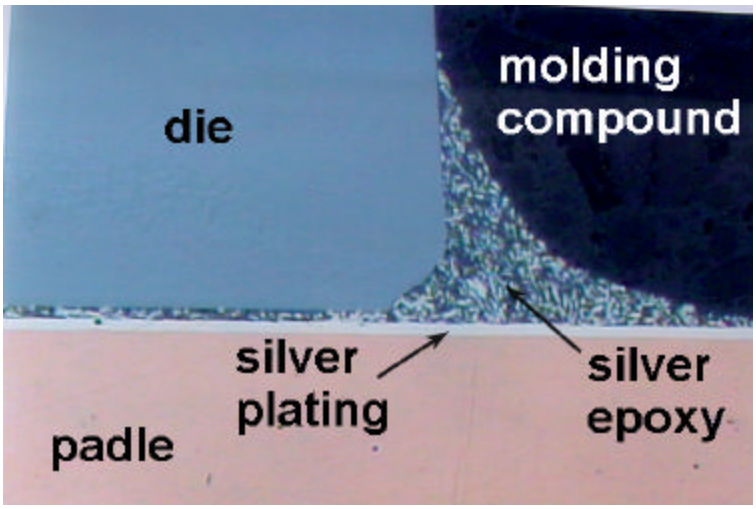

Figure 16. Close-up of the die attachment. (200X)

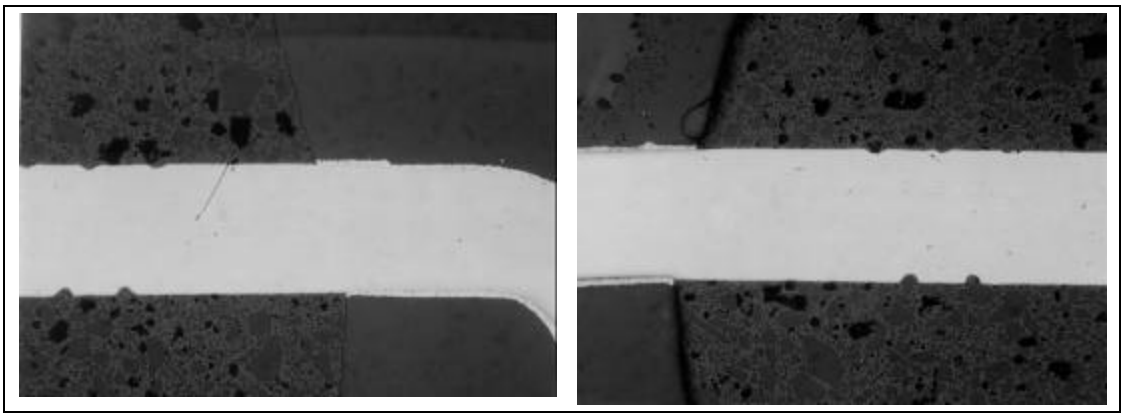

Figure 17. Close-up of the lead entries. (100X).

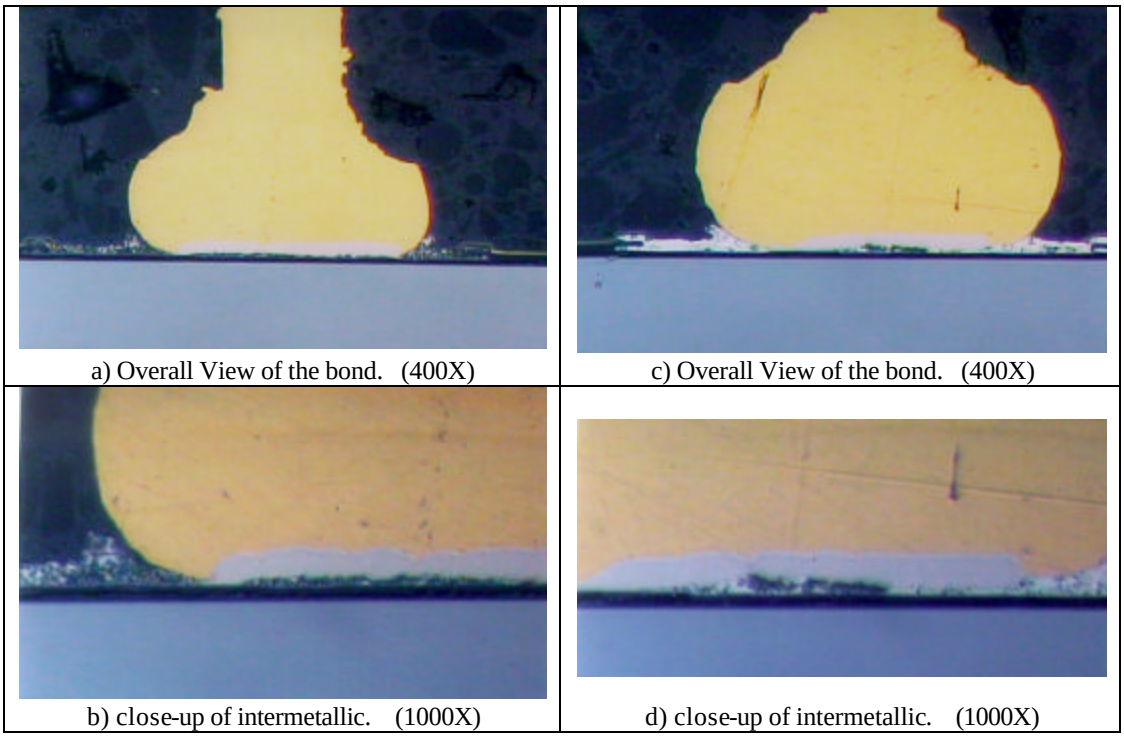

a) Overall View of the bond. (400X)

c) Overall View of the bond. (400X)

b) close-up of intermetallic. (1000X)

d) close-up of intermetallic. (1000X)

Figure 18. Cross-section of two wire bonds showing adequate Au/Al intermetallic formation.